Correlation-hole method for the spectra of superconducting microwave billiards

H. Alt,[1] H.-D. Gräf,[1] T. Guhr,[2] H. L. Harney,[2] R. Hofferbert,[1] H. Rehfeld,[1] A. Richter,[1] and P. Schardt[1,*]
[1]*Institut für Kernphysik, Technische Hochschule Darmstadt, D-64289 Darmstadt, Germany*
[2]*Max-Planck-Institut für Kernphysik, D-69029 Heidelberg, Germany*
(Received 17 June 1996; revised manuscript received 5 February 1997)

The spectral fluctuation properties of various two- and three-dimensional superconducting billiard systems are investigated by employing the correlation-hole method. It rests on the sensitivity of the spectral Fourier transform to long-range correlations and is thus an alternative technique to study chaotic dynamics. First, we apply the method to the eigenfrequencies that are extracted from the measured resonances. Second, we analyze the unfolded raw spectra, including the shape of the resonances. The merit of the method lies in a clear separation of the statistics due to the positions and due to the shape of the resonances. However, we show that statistical fluctuations of the intensities of the resonances have a strong impact on the observable. Therefore, the visibility of the correlation hole is studied as a function of the number of independent statistical variables entering into the intensities. The visibility improves if independent spectra are superimposed.
[S1063-651X(97)09306-9]

PACS number(s): 05.45.+b, 03.65.Ge, 41.20.Jb

I. INTRODUCTION

In recent years, the experimental study of chaotic dynamics in billiard systems has attracted considerable interest. Unlike nuclei, atoms, molecules, or solid-state probes, billiard systems can be specifically designed to investigate certain aspects of chaotic dynamics. This ''toy model'' feature, which the aforementioned systems lack, makes billiard systems very useful for studies of chaotic dynamics. Electromagnetic billiards simulating the corresponding quantum systems were experimentally investigated for the first time in Refs. [1–3]. The use of superconducting instead of normally conducting billiards yields an immense improvement in the quality of the measured spectra. Results were presented in Ref. [4].

The fluctuation properties of a rich variety of systems in nuclear, atomic, molecular, and solid-state physics have been studied experimentally and theoretically. In the case of fully developed chaos, they are found to be universal and very accurately described by random matrix theory [5–10]. Due to general symmetry constraints, a time-reversal invariant system with conserved or broken rotational invariance is modeled by the Gaussian orthogonal ensemble (GOE) or the Gaussian symplectic ensemble (GSE), while the Gaussian unitary ensemble (GUE) describes time-reversal noninvariant systems [6]. Regular systems, on the other hand, show significantly different fluctuation properties. Remarkably, they are, unlike the chaotic ones, not generic and can differ from system to system. Although one often encounters the complete lack of any correlations, which is referred to as Poisson regularity, the extreme opposite, i.e., the totally correlated spectrum of the harmonic oscillator, also falls into the regular class.

In order to study the fluctuation properties on short and long scales, one commonly analyzes the nearest-neighbor spacing distribution and the spectral rigidity [7,10]. This requires one to extract the positions of the levels from the measured spectrum. Thus the analysis is done on the so-called stick spectrum, i.e., the sequence of those eigenenergies or eigenfrequencies that could be identified in the raw spectra. However, one often has to deal with poorly resolved spectra, which prevents some levels from being found. This ''missing level effect'' has a considerable impact since it counterfeits correlations that do not exist. Fluctuation measures that are less sensitive to the missing level effect are therefore highly desirable.

In molecular physics, such a technique was developed by Leviandier *et al.* [11] for the analysis of the long-range correlations. The properly smoothed Fourier transform of the spectral autocorrelation function maps the long-range correlations onto short scales in Fourier space. As compared to fluctuations of regular systems, chaotic dynamics causes a considerable suppression of this Fourier transform near the origin, a so-called correlation hole. This has been experimentally observed in spectra of the molecules acetylene, methylglyoxal, and nitrogendioxyd [11,12]. Recently it was shown that nuclear spectra exhibit the correlation hole, too [11,13].

As pointed out already, fluctuation measures such as the nearest-neighbor spacing distribution or the spectral rigidity can only be used for the extracted stick spectrum. The correlation-hole method of Ref. [11], however, is also applicable to the raw spectra since the Fourier transform separates the statistics of the positions of the eigenenergies from the statistics of the intensities and widths. A possibly faulty and incomplete extraction of the positions and the widths from the spectra can thus be avoided. Consequently, the correlation-hole method is, in principle, less sensitive to the missing level effect and it is worthwhile to study its applicability to other physical systems.

The theory of the correlation hole for realistic spectra, i.e., including the linewidths, was worked out in Ref. [14] in the framework of a scattering model. In the same picture, the correlation hole observed by laser spectroscopy in methylglyoxal [11] was numerically simulated in Ref. [15]. A sum-

*Present address: Siemens AG, Bereich Medizinische Technik, D-91052 Erlangen, Germany.

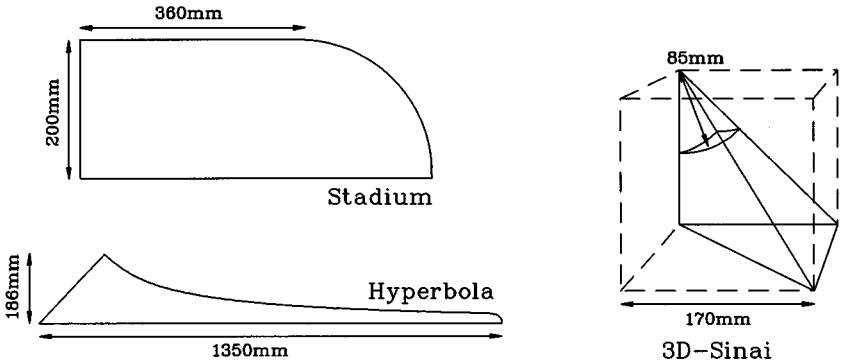

FIG. 1. Geometries of the superconducting resonators that were used in the experiments. Note that all systems are desymmetrized to avoid parity mixing. In comparison with the full systems, this yields a quarter stadium, an eighth of a hyperbola, and a 48th of a 3D Sinai billiard, respectively. In the case of the latter, the sides of the drawn cube are 170 mm long and the radius of the removed sphere measures half of this length, i.e., 85 mm.

mary and a qualitative discussion of the Fourier transform of statistical spectra can be found in Ref. [16]. A conspicuous short version of the theory of the correlation hole is presented in Appendix A of Ref. [17]. In Ref. [18], the correlation hole is related to its classical analog, the survival probability. The correlation-hole method was applied to billiard spectra by Kudrolli *et al.* [19]. However, these authors studied only the extracted stick spectra.

In the present work, we apply this method to the rich variety of billiard spectra that we have measured in recent years. We have two goals. First, we want to verify the significance of the correlation hole for billiards of quite different geometries by analyzing the stick spectra of the extracted levels. Second, we use the correlation-hole technique for the unfolded raw spectra and discuss the merits and the problems of such an analysis. We present a method of superimposing several raw spectra in order to improve upon the visibility of the correlation hole. The excellent resolution of the spectra measured in superconducting microwave cavities makes the recent data the ideal object for such an analysis.

After a short description of the experiment in Sec. II, we present the theoretical concepts in Sec. III. We perform the analysis of our data in Sec. IV and finish with conclusions in Sec. V.

II. EXPERIMENT

Due to the equivalence of the stationary Schrödinger equation for quantum systems to the corresponding Helmholtz equation for electromagnetic resonators in two dimensions, it is possible to simulate a quantum billiard of a given shape with the help of a sufficiently flat macroscopic electromagnetic resonator of the same shape [1–3]. We have experimentally studied several two- and three-dimensional (3D) billiard systems using superconducting microwave resonators made of niobium. Figure 1 shows some of the investigated cavities as well as their dimensions. Early experiments using superconducting instead of normally conducting resonators were performed in a desymmetrized Bunimovich stadium billiard and a truncated hyperbola billiard [4,20,21] using the 2-K cryostats of a superconducting electron linear accelerator described by Auerhammer *et al.* [22]. Recently, a desymmetrized 3D Sinai billiard [23,24] was experimentally investigated in a different and very stable 4-K bath cryostat. Note that the electromagnetic Helmholtz equation is vectorial in three dimensions and cannot be reduced to an effective scalar equation. Thus it is structurally different from the scalar Schrödinger equation. It is of considerable interest that the statistical concepts developed in the theory of quantum chaos and random matrices are also applicable to arbitrary classical electromagnetic wave phenomena. Conceptually, this is similar to the study of spectral fluctuations of elastomechanical eigenmodes in aluminum [25,26] and quartz [27] blocks, which are also described very well by random matrix theory.

All resonators mentioned above were excited in the frequency range between 0 and 20 GHz using capacitively coupling dipole antennas sitting in small holes on the niobium surface. Using one antenna for the excitation of the resonator and either another or the same one for the detection of the microwave signal, we were able to measure the transmission or the reflection spectrum of the resonator, respectively, by employing a Hewlett Packard HP8510B vector network analyzer. As an example, Fig. 2 shows a typical transmission spectrum of the 3D Sinai billiard in the range between 6.50 and 6.75 GHz. The signal is given as the ratio of output power to input power on a logarithmic scale. The measured

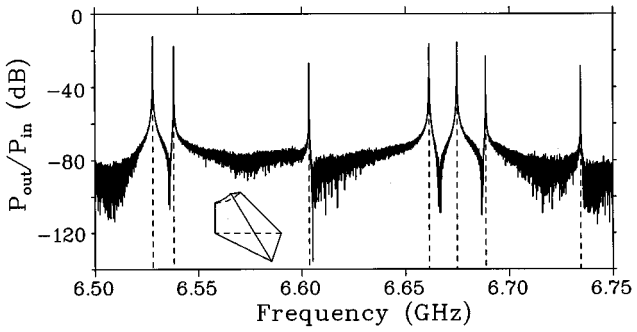

FIG. 2. Transmission spectrum of the 3D Sinai billiard in the range between 6.50 and 6.75 GHz. The signal is given as the ratio of output power to input power on a logarithmic scale. The dashed vertical lines mark the extracted eigenfrequencies f_μ as used in the stick spectrum.

resonances have quality factors of up to $Q \approx 10^7$ and signal-to-noise ratios of up to $S/N \approx 70$ dB, which makes it easy to separate the resonances from each other and from the background. As a consequence, all the important characteristics such as eigenfrequencies and widths can be extracted with a very high accuracy [21,28,29]. A detailed analysis of the original spectra yields a total number of approximately 1000 resonances for the 2D billiards (hyperbola and stadium) and nearly 1900 resonances for the 3D Sinai billiard. These eigenvalue sequences form the basis of the present test of the correlation-hole method.

III. THEORETICAL CONCEPTS OF THE CORRELATION-HOLE METHOD

We summarize, for the convenience of the reader, the basic ideas in Sec. III A and some earlier results on the two-level form factors in Sec. III B. We discuss the theoretical results on the correlation hole for stick and raw spectra in Secs. III C and III D, respectively.

A. Basic ideas

Consider a spectrum $I(E)$ or $I(f)$ measured as a function of energy E or, in our case, frequency f. This spectrum is described as a finite superposition of isolated or interfering resonances of a given universal shape $L(f)$ with statistically distributed positions, intensities, and widths. Although the shape is often known to be a Lorentzian [28,29], we keep the discussion general. In order to analyze the true fluctuations, one removes secular variations of the level density, i.e., the Weyl- or Thomas-Fermi contribution [30–32]. To this end, one introduces [7] the smooth part $N^{\mathrm{Weyl}}(f)$ of the integrated level density as the new coordinate by setting $x = N^{\mathrm{Weyl}}(f)$ for our experimental and theoretical discussions. Since we wish to study generic fluctuations, we shall henceforth assume that this unfolding procedure has been performed and write $I = I(x)$. This implies that, in the variable x, the mean level spacing is unity everywhere.

Hence we study a spectrum of N levels x_μ, $\mu = 1, \ldots, N$, on this unfolded scale. In the following, the level number N is always assumed to be large. To simplify the theoretical description, we make the further assumption that the line shape $L(x)$ does not depend on the intensities y_μ for a given resonance μ in the expression

$$I(x) = \sum_{\mu=1}^{N} y_\mu \, L(x - x_\mu), \tag{1}$$

where the line shape is normalized to unity. The observable of interest is the decay function, i.e., the modulus squared of the Fourier transform of the spectrum

$$|C(t)|^2 = \left| \int_{-\infty}^{+\infty} dx I(x) \exp(2\pi i x t) \right|^2. \tag{2}$$

The Fourier coordinate t defines an unfolded time. This expression can be rewritten as the Fourier transform

$$|C(t)|^2 = \int_{-\infty}^{+\infty} d\omega A(\omega) \exp(2\pi i \omega t) \tag{3}$$

of the autocorrelation function

$$A(\omega) = \int_{-\infty}^{+\infty} d\Omega I(\Omega - \omega/2) I(\Omega + \omega/2). \tag{4}$$

At this point a comment on the assumed independence of the line shape $L(x)$ of the intensities y_μ is in order. From scattering theory [33] it is known that this is the case only if the number Λ of open decay channels is very large. Strictly speaking, this is not true for the experiments to be analyzed here. The decay channels are the antennas that couple the cavity to the external world and hence $\Lambda = 2-4$; see the discussion below. However, the assumption of independence is to some extent justified here since it affects only the long-time behavior of the decay function $|C(t)|^2$, whereas the correlation hole is a feature found in the short-time behavior. Moreover, the more general theory also shows that the neglect of interference effects as done in Eq. (1) is justified. Thus, it turns out that our simplification still yields a satisfactory description of the correlation hole in all cases we studied.

Replacing the energy average in Eq. (4) by the average over an ensemble of resonances, one can make use of two results of random matrix theory [5,6,21]: (i) the y_μ are independent of the x_μ and (ii) for $\mu \neq \nu$ the intensities y_μ, y_ν are independent of each other. The function (4) then can be cast into the form

$$\begin{aligned} A(\omega) = N\overline{y^2} \int_{-\infty}^{+\infty} dx' L(\Omega - \omega/2 - x') L(\Omega + \omega/2 - x') \\ + N\overline{y^2} - N\overline{y}^2 \int_{-\infty}^{+\infty} dx' \int_{-\infty}^{+\infty} dx'' L(\Omega - \omega/2 - x') \\ \times L(\Omega + \omega/2 - x'') Y_2(x'' - x'). \end{aligned} \tag{5}$$

Here $Y_2(x)$ denotes the Dyson-Mehta two-level cluster function [6]. It describes the two-point correlations; more precisely, $[1 - Y_2(x)]dx$ is the probability to find two resonances separated by the distance x on the unfolded scale. Thus, for large arguments x, the correlations have to disappear and $Y_2(x)$ approaches zero. Note that $\overline{y}^2$, the square of the first moment of the intensities, and $\overline{y^2}$, the second moment, appear in Eq. (5).

We introduce the Fourier transform of the two-level cluster function,

$$b_2(t) = \int_{-\infty}^{+\infty} dx Y_2(x) \exp(2\pi i x t), \tag{6}$$

and analogously the Fourier transform $\widetilde{L}(t)$ of the line shape $L(x)$. The function $b_2(t)$ is referred to as the two-level form factor [6]. Just like the two-level cluster function, it has to vanish for large arguments t. Since the last term on the right-hand side of Eq. (5) contains a convolution, we can make use of the convolution theorem to evaluate the Fourier transform of $A(\omega)$. Collecting everything, one finds [11,14,16,17] for non-negative times

$$|C(t)|^2 = N\overline{y^2}\,\delta(t) + N\overline{y^2} |\widetilde{L}(t)|^2 [1 - \alpha b_2(t)], \tag{7}$$

where we denote the ratio of the statistical moments by

$$\alpha = \overline{y^2}/\overline{y^2}. \tag{8}$$

The correlation hole is described by the function $[1-\alpha b_2(t)]$, while $|\tilde{L}(t)|^2$ describes the decay of the resonances. Thus the statistics of the positions is separated from the statistics of the intensities. The δ function in Eq. (7) occurs since we assumed N to be very large. For a finite number of levels, this contribution will acquire a width as discussed in detail in Refs. [14,17]. Due to the high number of levels in our data, we disregard this contribution in the following.

If the resonances are well isolated, then $|\tilde{L}(t)|^2$ varies much more slowly than $b_2(t)$. In the extreme case of vanishing widths, i.e., $L(x)=\delta(x)$, the function (7) approaches $N\overline{y^2}$ for large times t. For the more realistic Lorentzian line shape [28,29] one has $\tilde{L}(t)=\exp(-\pi\Gamma t)$, where Γ is the total width, implying that the function (7) decays exponentially.

B. Correlation hole and two-level form factors

For the convenience of the reader, we collect here the well-known results for the form factors $b_2(t)$ introduced in Eq. (6). The case that the positions x_μ, x_ν of any two different resonances $\mu \neq \nu$ are completely uncorrelated is referred to as Poisson regularity [6,7]. Obviously, the two-level cluster function must be zero everywhere, $Y_2^{\text{Poisson}}(x)=0$, and therefore also $b_2^{\text{Poisson}}(t)=0$, which results in $|C(t)|^2 \approx N\overline{y^2}=\text{const}$ even for small values of t. There is no correlation hole.

In the case of fully developed chaos, the statistics of the positions is described by the Gaussian ensembles [6]. The general symmetry constraints imply that a time-reversal invariant system with conserved or broken rotational invariance is modeled by the Gaussian orthogonal or the symplectic ensemble, while the Gaussian unitary ensemble describes time-reversal noninvariant systems. We summarize the results for the form factors [6]. The situation most commonly encountered is described by the GOE, yielding

$$b_2^{\text{GOE}}(t)=\begin{cases} 1-2t+t\ln(1+2t), & 0<t\leqslant 1 \\ -1+t\ln[(2t+1)/(2t-1)], & t>1. \end{cases} \tag{9}$$

This function is displayed in Fig. 3. It corresponds to a decay function (7) for $\alpha=1$, which has been normalized by $N\overline{y^2}$. The GSE form factor is given by

$$b_2^{\text{GSE}}(t)=\begin{cases} 1-t/4+(t\ln|1-t|)/4, & 0<t\leqslant 2 \\ 0, & t>2 \end{cases} \tag{10}$$

and thus exhibits a divergence at $t=1$. Importantly, for all fully chaotic cases, we have for vanishing times $b_2(0)=1$. Thus, according to Eq. (7), the deepest point of the correlation hole is reached for small values of the time t and has the value $|C(t)|^2 \approx N\overline{y^2}(1-\alpha)$.

C. Stick spectra

Suppose that all resonances have a vanishing width, i.e., we consider a sequence of levels at positions x_μ represented by δ functions. If, moreover, all of them have the same intensity, $y_\mu=\overline{y}$, Eq. (1) reduces to

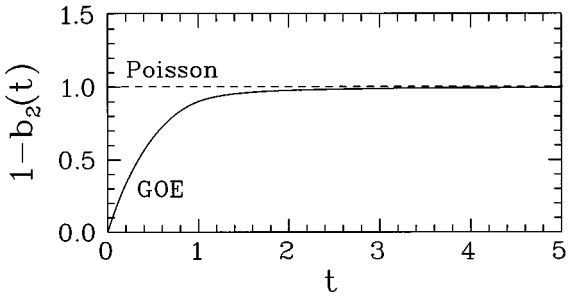

FIG. 3. The phenomenon of the correlation hole due to the two-level form factor is clearly visible for small values of t. The function $1-b_2(t)$ is displayed for the cases of Poisson and GOE statistics according to Eq. (9).

$$I(x)=\overline{y}\sum_{\mu=1}^{N}\delta(x-x_\mu), \tag{11}$$

which is nothing but the spectral function. It serves as the mathematical definition of the term ''stick spectrum'' [12]. Formally, the probability distribution of the intensity y_μ is given by a δ distribution, which implies $\overline{y^2}=\overline{y^2}$; hence, according to the definition (8), we find $\alpha=1$. Consequently, the function $|C(t)|^2$ of Eq. (7) becomes

$$|C(t)|^2=N\overline{y^2}[\delta(t)+1-b_2(t)]. \tag{12}$$

This is the case of maximum visibility of the correlation hole. For a realistic distribution $p(y)$ of the intensities, we will always find values of α that are smaller, often considerably smaller, than unity.

D. Correlation hole for raw spectra

The typical raw spectra of our resonators can be described as a superposition of isolated Lorentzian resonances [28,29] with statistically distributed locations, intensities, and widths. This closely parallels the situation of isolated resonances in a compound nucleus scattering experiment [33]. Due to a minimized surface resistance in the superconducting billiards, the total width is basically composed of a sum over partial widths that describe the power dissipation into the Λ decay channels realized by the antennas. Thus each total width is given by

$$\Gamma_\mu=\sum_{c=1}^{\Lambda}\Gamma_{\mu c} \tag{13}$$

for every resonance labeled by μ and channels denoted by c. The small number of decay channels Λ in our experiments, i.e., $\Lambda=2-4$, leads to a set of strongly fluctuating widths Γ_μ. We remark that this allows us to examine quantum phenomena such as the nonexponential decay of the spectral autocorrelation function [21].

The simplified theoretical model that was introduced in Sec. III A, however, is by construction not suited to describe this general case, but rather explains spectra of systems with

a constant total width. This situation can arise due to a high number of decay channels [33] or due to certain peculiarities of the physical system or the measurement [11,15]. As mentioned above, the present simplification concerns the long-time behavior of $|C(t)|^2$ and not the correlation hole that shows up on short-time scales. This simplification is not valid if there are sizable correlations between the intensities y_μ and the total widths Γ_μ. Therefore, in the present discussion, it is sufficient to assume a realistic distribution for the intensities y_μ. This defines an adequate model for raw spectra and has to be viewed in contrast to the δ distribution of the intensities y_μ considered in Sec. III C. It should be emphasized that we neglect, for reasons of consistency, interference terms between the individual resonances. Hence, in the terminology of scattering theory, our model applies to the case of isolated resonances.

If the spectrum $I(x)$ has been measured in reflection in, say, channel a, the intensities y_μ of the μth resonance are given by

$$y_\mu = \Gamma_{\mu a}\,, \tag{14a}$$

where $\Gamma_{\mu a}$ is the partial width of the resonance with respect to the channel, i.e., the antenna, a. Experiments as well as the theory of random matrices show that the partial widths are distributed according to a Porter-Thomas law [5,6,21], which describes a fully chaotic system, resulting in

$$\alpha = \tfrac{1}{3}\,. \tag{14b}$$

If, however, the spectrum $I(x)$ has been measured in transmission from channel a to, say, channel b, the intensities y_μ are given by the products

$$y_\mu = \Gamma_{\mu a}\,\Gamma_{\mu b} \tag{15a}$$

of the partial widths with respect to the entrance and exit channels. Taking $\Gamma_{\mu a}$ and $\Gamma_{\mu b}$ to be statistically independent variables with Porter-Thomas distributions one arrives at

$$\alpha = \tfrac{1}{9}\,. \tag{15b}$$

These two values of α simply reflect a Gaussian distribution for the decay amplitudes that is at the core of the Porter-Thomas law.

Hence, as indicated already, the statistical fluctuations of the weight y more or less suppress the correlation hole. The δ distribution considered in Sec. III C is much more favorable for the visibility of the correlation hole than a realistic distribution that will always give $\alpha<1$. Reducing these fluctuations would restore the correlation hole. This can be achieved by the superposition of statistically independent spectra. Suppose that spectra have been measured via all, or all possible, combinations of the Λ antennas attached to a given resonator. The positions x_μ of the resonances are the same in all spectra; the intensities y_μ, however, vary from spectrum to spectrum. Thus the intensities of the spectrum obtained from superimposing all these spectra will fluctuate much less. In the limit of a superposition of infinitely many spectra, all intensities will be the same and we are back to the case of the stick spectrum.

We want to make this argument more quantitative. First, we discuss reflection measurements. We write the μth intensity of the superposition of all possible reflection spectra in the form

$$y_\mu = \sum_{a=1}^{\Lambda} \Gamma_{\mu a}\,. \tag{16a}$$

Under the assumptions that $\Gamma_{\mu a}$ has Porter-Thomas statistics and that the average value is independent of μ we find

$$\alpha = \frac{\Lambda}{\Lambda+2}\,. \tag{16b}$$

For $\Lambda=1$ one recovers the result (14b) and, as expected, this expression approaches unity for large Λ.

Second, we turn to transmission measurements. Adding up all possible transmission spectra, we obtain the μth intensity

$$y_\mu = \frac{1}{2}\sum_{\substack{a,b=1\\ a\neq b}}^{\Lambda} \Gamma_{\mu a}\,\Gamma_{\mu b}\,. \tag{17a}$$

Under the same assumptions as above this leads to

$$\alpha = \frac{\Lambda-1}{\Lambda+7}\,. \tag{17b}$$

Again, this is consistent with the result (15b) for $\Lambda=2$. Moreover, for large Λ, the expression (17b) approaches unity, as it should.

IV. APPLICATION TO EXPERIMENTAL DATA

After some general considerations in Sec. IV A, we present the analysis of stick and raw spectra in Secs. IV B and IV C, respectively.

A. General considerations

The Fourier transform $C(t)$ of the measured spectrum $I(x)$ does still contain all the information. As is well known, if the experimental data consist of many levels in a sufficiently long interval, the Fourier transform can, before unfolding, be used to obtain information about the periodic orbits of the system [34] that manifest themselves in a rich structure consisting of many peaks. Here, however, we aim at an understanding of the generic statistical features of our experimental data. In other words, since we are not interested in resolving individual properties such as periodic orbits, we have to average over all realizations of the physical system in question. This, however, is precisely what random matrix theory did for us when we went from the autocorrelation function (4) to its ensemble average. According to Delon *et al.* [12] the ensemble average can be simulated by applying a smoothing procedure to the experimental decay function $|C(t)|^2$. It turns out [12] that the most appropriate procedure is a convolution of $|C(t)|^2$ with a Gaussian. Hence we have to compare the theoretical results to the function

$$\langle |C(t)|^2 \rangle = \int_{-\infty}^{+\infty} dt' |C(t')|^2 \frac{1}{\sqrt{2\pi\sigma_t^2}} \exp\left(-\frac{(t-t')^2}{2\sigma_t^2} \right), \tag{18}$$

where the variance σ_t was chosen to depend on the time as $\sigma_t = t/10$. This procedure is referred to as ''full Gaussian smoothing.''

B. Correlation hole for stick spectra

We now analyze the sequences of levels that were extracted from the measured spectra, i.e., the stick spectra. In some cases, we perform an additional test of GOE characteristics following the discussion of Ref. [13]. A theorem due to Dyson and Mehta [35] states that if one takes a GOE spectrum $\{f_1, f_2, f_3, \ldots\}$ and divides it into two sequences of odd and even indices, i.e., into $\{f_1, f_3, f_5, \ldots\}$ and $\{f_2, f_4, f_6, \ldots\}$, then each of these two spectra obeys, after proper unfolding, the GSE statistics. Following this idea, the experimentally found stick spectrum was divided into two equivalent sets with half the number of eigenfrequencies, put together sequentially, and the whole analysis was repeated. The theoretical prediction is given by using Eq. (10) in the expression (12). In contrast to the GOE case, the GSE form factor $b_2(t)$ has a singularity at $t=1$ due to the different oscillatory structure of the two-level correlation function $Y_2(x)$. Thus one expects a characteristic peak in the function $\langle |C(t)|^2 \rangle$ at this time t, which gives information on correlations on the scale of about two mean level spacings. As pointed out in Ref. [13], the decay function constructed in this way by omitting every other level contains information on higher than two-level correlations of the original spectrum.

In Secs. IV B 1 and IV B 2, we discuss the hyperbola and the stadium billiard, respectively. In Sec. IV B 3, we analyze the stick spectrum of the 3D Sinai billiard.

1. Hyperbola billiard

The upper part of Fig. 4 shows the result for the measured spectrum of the hyperbola-billiard whose shape is displayed in Fig. 1. The full line is the experimental result for $\langle |C(t)|^2 \rangle$ according to Eq. (18).

Since the hyperbola billiard has been proven [36,37] to be fully chaotic in the classical limit, one expects [38] to find GOE fluctuations in the spectrum. Indeed, as Fig. 4 shows, the agreement with the theoretical prediction of Eq. (12) with $b_2(t)$ given by Eq. (9) is very good. Note that $\langle |C(t)|^2 \rangle$ and Eq. (12) have been divided by $N\overline{y^2}$ to allow a comparison with Fig. 3.

The test of GSE statistics according to the Dyson-Mehta observation mentioned above yields the curve shown in the lower part of Fig. 4. Again, the agreement with the theory is good. Here, to be consistent, we have smoothed the theoretical curve, too, with the help of Eq. (18). We do not exclude the possibility that the discrepancy between this curve and the experimental result at $t=1$ might hint at deviations of the higher-order and the medium-range correlations in the spectrum from the GOE prediction. Due to the limited amount of data, however, we cannot perform more detailed tests, which would be necessary to make a definite statement.

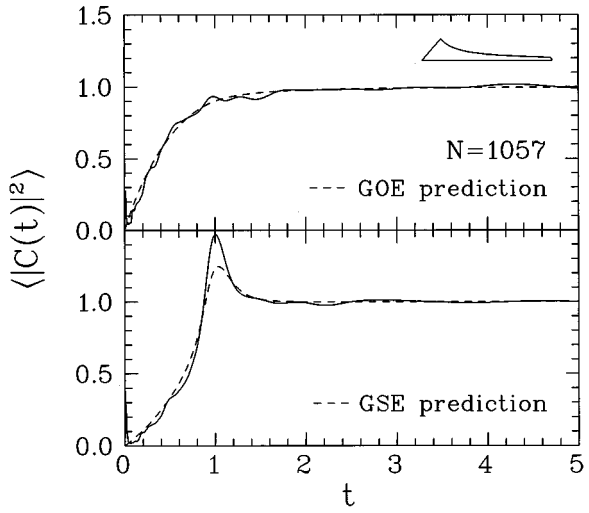

FIG. 4. Function $\langle |C(t)|^2 \rangle$ for the stick spectrum of the hyperbola billiard. Note that the ordinate is divided by $N\overline{y^2}$ in order to allow an immediate comparison with Fig. 3 by using Eq. (12). The full line is the experimental result and the dashed line the theoretical result.

2. Stadium billiard

The Bunimovich stadium billiard [39] displayed in Fig. 1 is also totally chaotic in the classical sense, but it has an additional feature: In contrast to the hyperbola, the stadium possesses one neutrally stable and nonisolated periodic orbit, the so-called bouncing ball orbit that propagates between the two straight and parallel segments of the geometry. This lends a certain type of regular characteristics to the system. Thus, in calculating $\langle |C(t)|^2 \rangle$, we test the influence of this remaining regularity on the correlation hole. The result is given in Fig. 5, where in the lower part the bouncing ball orbit has been removed by extracting the term that the bouncing ball orbit contributes to the smooth part of the level

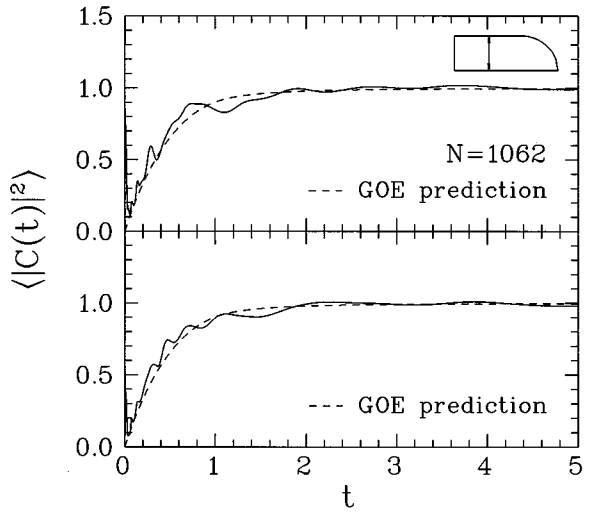

FIG. 5. Function $\langle |C(t)|^2 \rangle$ for the stick spectrum of the stadium billiard, as in Fig. 4. The experimental curve (solid line) in the upper part includes the bouncing ball contribution. In the lower part, the bouncing ball contribution has been removed. The theoretical prediction (dashed line) is the same in both cases.

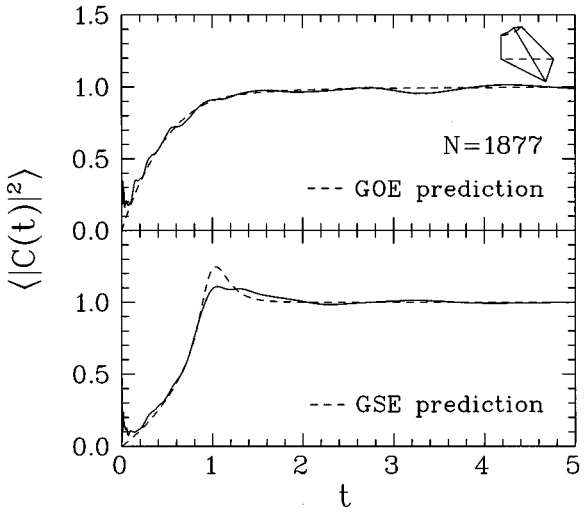

FIG. 6. Function $\langle|C(t)|^2\rangle$ for the stick spectrum of the 3D Sinai billiard, as in Fig. 4.

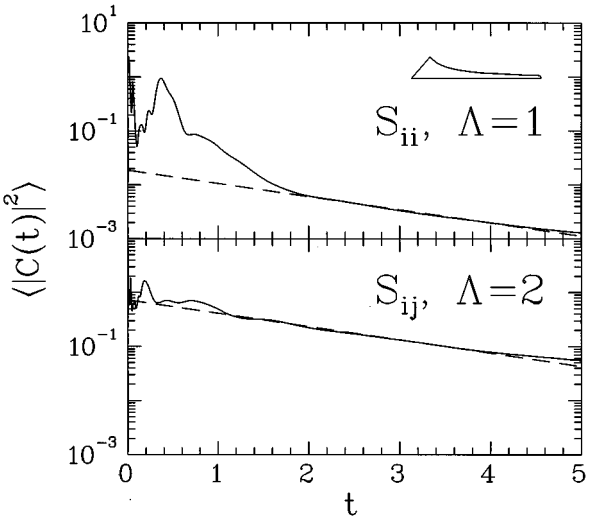

FIG. 7. Function $\langle|C(t)|^2\rangle$ for original raw spectra of the hyperbola billiard. The two parts of the figure show the result from a spectrum measured in reflection (S_{ii}) and one measured in transmission (S_{ij}). The scale of the ordinate is discussed at Eq. (19).

density [40] together with the common Weyl contribution in the unfolding procedure. As can be seen from the figure, this extraction amounts to a very slight correction towards the pure GOE characteristics. Due to the mapping of long-range spectral properties onto short times, the correlation hole is quite insensitive to the bouncing ball orbit.

3. 3D Sinai billiard

Finally, we have considered a spectroscopic system that generalizes the statistical concepts of quantum chaos in the sense that, although it does not represent or simulate a quantum system, its spectral features are found to coincide with GOE characteristics. As in the case of elastomechanical eigenmodes [25–27], this indicates that many classical wave phenomena might follow the predictions of random matrix theory. The system at hand is the 3D Sinai billiard [23,24,26,27] shown in Fig. 1. Its wave dynamics is described in terms of the vectorial Helmholtz equation in three dimensions. The resulting function $\langle|C(t)|^2\rangle$ is displayed in Fig. 6. As in the case of the hyperbola billiard, we also performed the GSE test on our data.

Note that, in this geometry, the eigenvalues of the quantum-mechanical Schrödinger equation as well as the eigenvalues of the vectorial electromagnetic Helmholtz equation show, due to the bouncing ball orbits, slight deviations from pure GOE behavior [23] in other statistics such as the number variance Σ^2 or the spectral rigidity Δ_3. It is not possible to draw direct conclusions from that to the present system since the ray limit of the vectorial Helmholtz equation is different from the classical limit of the Schrödinger equation. However, it could be speculated that the influence of the corresponding bouncing ball orbits in the present system is suppressed due to an effective average over all their different lengths. In any case, the effect of the bouncing ball orbits becomes visible at comparatively large lengths in the spectrum. Thus, in our observable, it cannot be extracted with statistical significance since the Fourier transform maps it onto values of t that are of the order of the inverse length in the spectrum. Remember that the correlation hole is found at values of t that are roughly of the order unity. Nevertheless, a suppression of the peak at $t=1$ in the experimental curve is seen in the GSE test in the lower part of Fig. 6. One might be tempted to interpret this as due to those effects. Again, more detailed tests would require more data and, in this particular case, a thorough theoretical discussion of the ray limit of the vectorial Helmholtz equation too.

C. Raw spectra

As far as the stick spectra are concerned, the phenomenon of the correlation hole is obviously well understood. The agreement with theoretical predictions for all considered systems is satisfactory. We now apply the method to original and idealized raw spectra in Secs. IV C 1 and IV C 2, respectively. In Sec. IV C 3, the influence of certain statistical fluctuations on our findings is discussed and demonstrated using synthetic spectra.

1. Original raw spectra

We analyze original raw spectra of the hyperbola with a total number of $\Lambda=3$ antennas. Besides the unfolding, no further preparation has been performed. On Fig. 7, the function $\langle|C(t)|^2\rangle$ is shown for raw spectra of the hyperbola billiard. The ordinate is in principle as in Figs. 4–6: The function $\langle|C(t)|^2\rangle$ is given in units of $N\overline{y^2}$ in order to allow an immediate comparison with Fig. 3 and all other similar figures; see Eq. (7). It is, however, not obvious how to obtain $N\overline{y^2}$ from a spectrum unless one identifies and analyzes all the resonances. We proceed as follows.

If one assumes the line shape $L(x)$ to be a Lorentzian with width Γ, then the integral over the square of the spectrum $I(x)$ of Eq. (1) is

$$\int_{-\infty}^{+\infty} I^2(x)dx = \frac{4\pi}{\Gamma^3}\sum_{\mu=1}^{N} y_\mu^2 \approx 4\pi\frac{N\overline{y^2}}{\Gamma^3}. \tag{19}$$

This quantity is obtained by numerical integration. The width Γ is obtained by a fit procedure from the exponential decay

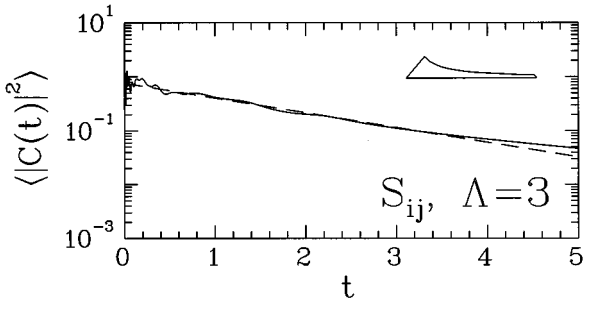

FIG. 8. Function $\langle|C(t)|^2\rangle$ for three superposed transmission spectra of the hyperbola. The scale of the ordinate is discussed at Eq. (19).

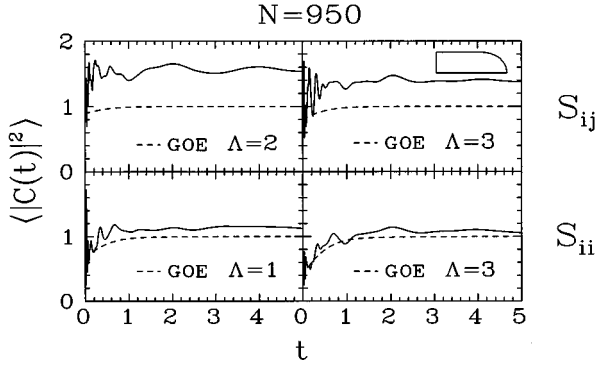

FIG. 9. Function $\langle|C(t)|^2\rangle$ for an idealized raw spectrum of the stadium billiard, as in Fig. 4. See the detailed explanation in the text. The experimental curves are given as solid lines, the theoretical ones as dashed lines.

of $\langle|C(t)|^2\rangle$ for $t>1$ as is illustrated by Fig. 7. See also the discussion at the end of Sec. III A. From these two pieces of information, Eq. (19) yields $N\overline{y^2}$.

In the upper part of Fig. 7, the function $\langle|C(t)|^2\rangle$ is shown for a raw spectrum of the hyperbola measured in reflection mode. Unfortunately, this function cannot be interpreted in terms of the correlation hole because it is dominated, up to $t\approx 2$, by a background that is typical for the reflection measurements. Since the radio-frequency cables we used for the transmission between source and resonator are interrupted by certain nonideal cable connectors, the measured frequency spectrum is modulated by the signal that is generated through reflections at these connectors and the resonator; see the oscillations of the spectral background in Fig. 1 of Ref. [21]. Furthermore, the size of the resonators and the lengths of the cables are of the same order. Therefore, the period of this spectral modulation is of the order of the mean level spacing and the power spectrum between $t=0$ and $t\approx 2$ is dominated by this artificial background peak. Note, however, that this does not at all preclude the analysis of every given resonance because Γ is very small compared to the period of the above oscillations.

The transmission spectra are free from that problem. Nevertheless, the correlation hole is not visible in the lower part of Fig. 7, where $\langle|C(t)|^2\rangle$ is given for a raw spectrum of the hyperbola measurement in transmission mode. At the place of the correlation hole, one observes fluctuations that will be discussed in Sec. IV C 3 below. They are due to the statistical fluctuations of the intensities y_μ. Note that the value of $\alpha=1/9$, expected from Eq. (15b) for this case, leaves little hope to see the correlation hole. According to Sec. III D, the value of α should improve if several spectra are superimposed. We have done so for all transmission spectra ($\Lambda=3$) of the hyperbola. According to Eq. (17b), one then expects $\alpha=1/5$. Figure 8 shows that this is not enough. Compared to the lower part of Fig. 7, the fluctuations are more suppressed, but the hole itself cannot be identified.

2. Idealized raw spectra

In order to acquire a deeper understanding of the statistical effects that are important for the correlation-hole method, we study ''idealized raw spectra.'' They are obtained by providing the experimentally found stick spectra with realistic intensities: We use the experimentally determined spectral properties of the stadium billiard with $\Lambda=3$ channels, i.e., the full set of parameters for the first 950 resonances including their positions x_μ as well as three sets of partial widths $\Gamma_{\mu c}$, which were shown to obey the Porter-Thomas distribution [21]. Note that these partial widths have been separately normalized to unity for each channel, i.e., $\langle\Gamma_{\mu c}\rangle=1$. The resulting functions $\langle|C(t)|^2\rangle$ for different cases are given in Fig. 9. In the upper half of the figure, transmission spectra S_{ij} for $i\neq j$ are analyzed. In the upper left part, a single transmission spectrum is used. This means $\Lambda=2$ in Eq. (17) and the theory predicts $\alpha=1/9$. In the upper right part, three transmission spectra have been superposed, i.e., $\Lambda=3$, and the prediction is $\alpha=1/5$. In the lower half of the figure, reflection spectra S_{ii} are analyzed. A single reflection spectrum is used in the lower left part. This means $\Lambda=1$ in Eq. (16), yielding $\alpha=1/3$. In the lower right part, $\Lambda=3$ reflection spectra have been superposed and Eq. (16) predicts $\alpha=3/5$. Note, in addition, that $\langle|C(t)|^2\rangle$ and the function in Eq. (7) were divided by $N\overline{y^2}$. Obviously, there is a strong deviation between the experimental and the theoretical curve in the case of the single spectra in the left column of Fig. 9. For the superpositions, this deviation is reduced.

3. Statistical fluctuations of the squared intensities and their impact

To give a qualitative interpretation of this deviation, we study the statistical fluctuations of $|C(t)|^2$ in the long-time limit $t\to\infty$, where the power spectrum is free of effects due to level clustering. We will show that the deviation just observed can be attributed to, at first sight unexpectedly, large statistical fluctuations of the squared intensities in the spectra. From Eqs. (1) and (2) with $L(x)=\delta(x)$ one obtains

$$|C(t)|^2=\sum_{\mu=1}^{N} y_\mu^2+\sum_{\substack{\mu,\nu=1\\ \mu\neq\nu}}^{N} y_\mu y_\nu \exp[2\pi i(x_\mu-x_\nu)t]. \quad (20)$$

In the limit $t\to\infty$ and due to the full Gaussian smoothing, the strongly fluctuating second term of this expression is suppressed. We define this limit as

$$X=\lim_{t\to\infty}\langle|C(t)|^2\rangle=\sum_{\mu=1}^{N} y_\mu^2. \quad (21)$$

The aforementioned ensemble average in the limit $N\to\infty$ yields the quantity

$$\overline{X}=\lim_{N\to\infty} X=N\overline{y^2}, \tag{22}$$

which is exactly the expression we used for the normalization in the previous analysis of the idealized raw spectra. Now, to estimate the statistical fluctuations of X, we have to calculate its second moment $\overline{X^2}$ and the relative standard deviation

$$\delta_{\rm rel}X=\sqrt{\frac{\overline{X^2}-\overline{X}^2}{\overline{X}^2}}. \tag{23}$$

In the case of a single transmission spectrum S_{ij} with $\Lambda=2$, one has $y_\mu=\Gamma_{\mu a}\Gamma_{\mu b}$, which yields

$$\delta_{\rm rel}X=\frac{1}{\sqrt{N}}\sqrt{\frac{\overline{\Gamma^4}^2}{\overline{\Gamma^2}^4}-1}. \tag{24}$$

This behaves, as expected, like $1/\sqrt{N}$. However, since the partial widths are Porter-Thomas distributed, the higher-order moments of Γ_μ obey

$$\overline{\Gamma^k}=(2k-1)!!\,\overline{\Gamma^k}, \tag{25}$$

implying that the statistical fluctuations strongly increase with the order of the statistical moment due to the factor $(2k-1)!!$. In the present case of $N=950$ resonances one obtains $\delta_{\rm rel}X\approx 0.38$, which is in good agreement with the experimental curve given in Fig. 9. For an increasing number of channels Λ, this relative variance shrinks since the superposition reduces the fluctuations in the intensities y_μ. For vanishing fluctuations in the intensities, one has $\delta_{\rm rel}X=0$. Since the parameter α is generated through the statistical moments of the y_μ, both the normalization and the correlation hole itself approach the theoretical prediction only as the number of included open channels is increased.

Remarkably, a superposition of reflection spectra even for the small number of only $\Lambda=3$ open channels allows, in principle, a reobservation of the correlation hole since we have $\alpha=3/5$. For the superimposed transmission spectra with $\alpha=1/5$, the hole is still weak. This explains why the hole could not be observed in the superposition of the original transmission spectra of the hyperbola in Fig. 8. Unfortunately, the favorable behavior of the reflection measurements cannot be exploited because of the experimental artifact discussed in Sec. IV C 1.

In order to demonstrate the influence of the number Λ of open channels on the correlation hole and on the normalization, we have finally calculated several superpositions of synthetic spectra for the hyperbola. We used the experimental spectrum of the positions x_μ and up to $\Lambda=10$ numerically simulated spectra of Porter-Thomas distributed partial widths Γ_μ with $\langle\Gamma_{\mu c}\rangle=1$. Thus, in contrast to the idealized raw spectra of the Sec. IV C 2, where the amplitudes were taken from the measurement, the synthetic spectra contain numerically generated amplitudes. Figure 10 displays the results for $\Lambda=2$, 3, 5, and 10. Since we treated the spectra as measured

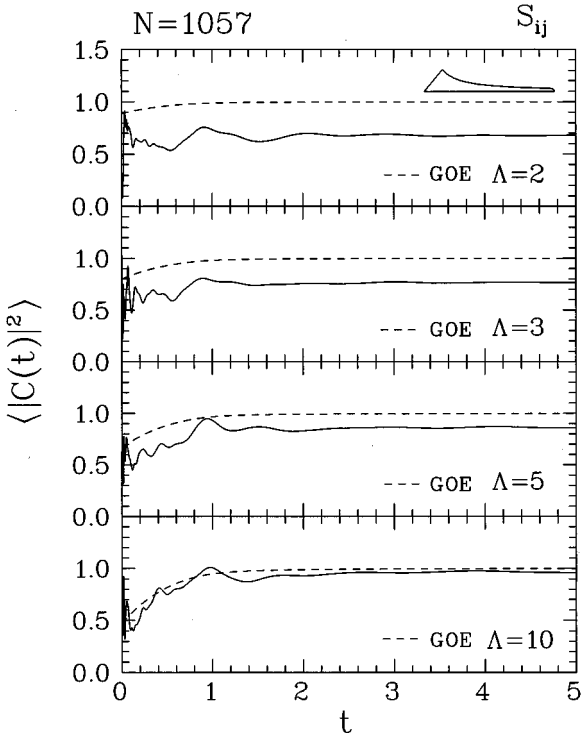

FIG. 10. Dependence of the visibility of the correlation hole on the number Λ of open channels for $\Lambda=2$, 3, 5, and 10. The scale of the ordinate is as in Fig. 4.

in transmission mode, we have, according to Eq. (17), ratios of the moments given by $\alpha=1/9$, 1/5, 1/3, and 9/17, respectively. Obviously, the systematic increase in Λ leads to a continuing reduction of the statistical fluctuations of y_μ, described by $\delta_{\rm rel}X$. For $\Lambda=10$ the agreement between the experimental and the theoretical curve is quite good. This demonstrates, for transmission and reflection measurements, how the correlation hole can be observed by superimposing independent spectra that individually do not show a significant correlation hole.

V. CONCLUSION

In the present work on the correlation-hole method, we have evaluated the decay function $\langle|C(t)|^2\rangle$ of stick spectra as well as that of original and idealized raw spectra for various two- and three-dimensional billiard systems. The stick spectra lead to the correlation hole as expected from random matrix theory. The nongeneric features implied by the presence of bouncing ball orbits in certain billiards did not affect the correlation hole in any observable way.

The fluctuations of the resonance intensities that are present in the raw spectra have a strong impact on the results. They decrease the visibility of the correlation hole. At the same time, they introduce fluctuations such that, even with approximately 1000 resonances in the spectrum, the decay function $\langle|C(t)|^2\rangle$ may fall quite far from its expected shape. This again precludes the observation of the correlation hole. It is, however, restored if sufficiently many spectra with statistically independent intensities are superimposed.

ACKNOWLEDGMENTS

We would like to thank H. Lengeler and the CERN workshops for the excellent fabrication of the niobium resonators. We are grateful to J. Nygård for helpful advice regarding the smoothing procedure of the Fourier transforms. We thank T. Gorin and I. Rotter for a very useful conversation. We also benefited from fruitful discussions with C. Dembowski and with C. Ianes Barbosa, who was supported from a grant of the Deutsche Akademische Austauschdienst during her stay in Darmstadt. T.G. acknowledges financial support from a Habilitanden-Stipendium of the Deutsche Forschungsgemeinschaft. This work has been supported by the Sonderforschungsbereich 185 ''Nichtlineare Dynamik'' of the Deutsche Forschungsgemeinschaft and in part by the Bundesministerium für Bildung und Forschung under Contract No. 06DA665I.

[1] H.-J. Stöckmann and J. Stein, Phys. Rev. Lett. **64**, 2215 (1990); J. Stein and H.-J. Stöckmann, *ibid.* **68**, 2867 (1992).
[2] E. Doron, U. Smilansky, and A. Frenkel, Phys. Rev. Lett. **65**, 3072 (1990).
[3] S. Sridhar, Phys. Rev. Lett. **67**, 785 (1991).
[4] H.-D. Gräf, H.L. Harney, H. Lengeler, C.H. Lewenkopf, C. Rangacharyulu, A. Richter, P. Schardt, and H.A. Weidenmüller, Phys. Rev. Lett. **69**, 1296 (1992).
[5] C.E. Porter, *Statistical Theories of Spectra: Fluctuations* (Academic, New York, 1965).
[6] M.L. Mehta, *Random Matrices*, 2nd ed. (Academic, San Diego, 1991).
[7] O. Bohigas and M.-J. Giannoni, in *Chaotic Motion and Random Matrix Theory*, edited by J. S. Dehesa, J. M. G. Gomez, and A. Polls, Lecture Notes in Physics Vol. 209 (Springer, Berlin, 1984), p. 1.
[8] O. Bohigas, in *Chaos and Quantum Physics*, edited by M.-J. Giannoni, A. Voros, and J. Zinn-Justin (Elsevier, Amsterdam, 1991), p. 89.
[9] M. Berry, in *Chaos and Quantum Physics* (Ref. [8]), p. 253.
[10] F. Haake, *Quantum Signatures of Chaos* (Springer, Berlin, 1991).
[11] L. Leviandier, M. Lombardi, R. Jost, and J.P. Pique, Phys. Rev. Lett. **56**, 2449 (1986).
[12] A. Delon, R. Jost, and M. Lombardi, J. Chem. Phys. **95**, 5701 (1991).
[13] M. Lombardi, O. Bohigas, and T.H. Seligman, Phys. Lett. B **324**, 263 (1994); C. R. Bybee, G. E. Mitchell, and J. F. Shriner, Z. Phys. A **335**, 327 (1996).
[14] T. Guhr and H.A. Weidenmüller, Chem. Phys. **146**, 21 (1990).
[15] U. Hartmann, H.A. Weidenmüller, and T. Guhr, Chem. Phys. **150**, 311 (1991).
[16] M. Lombardi, J.P. Pique, P. Labastie, M. Broyer, and T. Seligman, Comments At. Mol. Phys. **25**, 345 (1991).
[17] M. Lombardi and T.H. Seligman, Phys. Rev. A **47**, 3571 (1993).
[18] Y. Alhassid and N. Whelan, Phys. Rev. Lett. **70**, 572 (1993).
[19] A. Kudrolli, S. Sridhar, A. Pandey, and R. Ramaswamy, Phys. Rev. E **49**, R11 (1994).
[20] H. Alt, H.-D. Gräf, H.L. Harney, R. Hofferbert, H. Lengeler, C. Rangacharyulu, A. Richter, and P. Schardt, Phys. Rev. E **50**, 1 (1994).
[21] H. Alt, H.-D. Gräf, H.L. Harney, R. Hofferbert, H. Lengeler, A. Richter, P. Schardt, and H.A. Weidenmüller, Phys. Rev. Lett. **74**, 62 (1995).
[22] J. Auerhammer, H. Genz, H.-D. Gräf, R. Hahn, P. Hoffmann-Stascheck, C. Lüttge, U. Nething, K. Rühl, A. Richter, T. Rietdorf, P. Schardt, E. Spamer, F. Thomas, O. Titze, J. Töpper, and H. Weise, Nucl. Phys. A **553**, 841c (1993).
[23] H. Primack and U. Smilansky, Phys. Rev. Lett. **74**, 4831 (1995).
[24] H. Alt *et al.* (unpublished).
[25] R.L. Weaver, J. Acoust. Soc. Am. **85**, 1005 (1989).
[26] C. Ellegaard, T. Guhr, K. Lindemann, H.Q. Lorensen, J. Nygård, and M. Oxborrow, Phys. Rev. Lett. **75**, 1546 (1995).
[27] C. Ellegaard, T. Guhr, K. Lindemann, J. Nygård, and M. Oxborrow, Phys. Rev. Lett. **77**, 4918 (1996).
[28] H. Alt, P. von Brentano, H.-D. Gräf, R.-D. Herzberg, M. Philipp, A. Richter, and P. Schardt, Nucl. Phys. A **560**, 293 (1993).
[29] H. Alt, P. von Brentano, H.-D. Gräf, R. Hofferbert, M. Philipp, H. Rehfeld, A. Richter, and P. Schardt, Phys. Lett. B **366**, 7 (1996).
[30] H. Weyl, J. Reine Angew. Math. **141**, 1 (1912); **141**, 163 (1912).
[31] H. Weyl, J. Reine Angew. Math. **143**, 177 (1913).
[32] H.P. Baltes and E.R. Hilf, *Spectra of Finite Systems* (Bibliographisches Institut, Mannheim, 1975).
[33] C. Mahaux and H.A. Weidenmüller, *Shell-Model Approach to Nuclear Reactions* (North-Holland, Amsterdam, 1969).
[34] M.C. Gutzwiller, *Chaos in Classical and Quantum Mechanics* (Springer, New York, 1990).
[35] M.L. Mehta and F.J. Dyson, J. Math. Phys. **4**, 713 (1963).
[36] M. Sieber, Ph.D. thesis, Universität Hamburg, 1990.
[37] R. Aurich, T. Hesse, and F. Steiner, Phys. Rev. Lett. **74**, 4408 (1995).
[38] O. Bohigas, M.J. Giannoni, and C. Schmit, Phys. Rev. Lett. **52**, 1 (1984).
[39] L.A. Bunimovich, Zh. Eksp. Teor. Fiz. **89**, 1452 (1985) [Sov. Phys. JETP **62**, 842 (1985)].
[40] M. Sieber, U. Smilansky, S.C. Creagh, and R.G. Littlejohn, J. Phys. A **26**, 6217 (1993).